

# Electronic, Elastic Structure and Phase Stability of TaRu Shape Memory Alloys

A. A. Mousa<sup>1,\*</sup>, J. M. Khalifeh<sup>2</sup>, B. A. Hamad<sup>2</sup>

<sup>1</sup>Civil Engineer in Department, Middle East University, Amman, 11831, Jordan

<sup>2</sup>Physics Department, The University of Jordan, 11942, Amman, Jordan

**Abstract** The phase stability and electronic structure of TaRu shape memory alloys are studied using full-potential linearized augmented plane wave method (FP-LAPW) on the basis of the density functional theory (DFT). The calculated equilibrium volumes are about  $32 \text{ \AA}^3$  and  $30 \text{ \AA}^3$  for  $\beta$ -,  $\beta'$  and  $\beta''$  phases using the generalized gradient approximation (GGA) and local density approximation (LDA), respectively, in good agreement with the experimental values. The  $\beta''$ -phase is favored by about 85 meV/f.u. than the  $\beta$ -phase. The value of the density of states at the Fermi energy, confirms that the  $\beta''$  phase is the ground state equilibrium phase of TaRu at low temperatures, in agreement with the experimental findings.

**Keywords** Ta, Ru, DFT, Shape Memory Alloys, Bulk Modulus, Formation Energy

## 1. Introduction

Some metals that can remember their original shape and return to it when they are heated above a certain temperature are called the shape memory alloys (SMAs). The SMAs have two stable phases - the high-temperature phase, called *austenite* (the stronger high temperature phase) and the low-temperature phase, called *martensite* (the more deformable, lower temperature phase). Many SMAs have martensitic transformation below  $200^\circ \text{C}$  [1], so they are not suitable for high-temperature applications such as nuclear reactors, rockets and automotive engines [2]. So it is necessary to develop SMAs that have martensite transformation more than  $500^\circ \text{C}$ , called high temperature shape memory alloys [HTSMAs] [3, 4]. The HTSMAs are attracting scientists in the field of shape memory and superelastic technology. They are suitable for high-temperature applications such as those listed above [1, 2, 5, 6]. Tantalum Ruthenium (TaRu) is an example of such alloys [3]. These alloys exhibit ordered CsCl-type ( $Pm\bar{3}m$ ) cubic structure ( $\beta$ -phase) for temperatures above  $1100^\circ \text{C}$ . Below  $1100^\circ \text{C}$ , the crystal transforms to a tetragonal structure, called the  $\beta'$ -phase. When the temperature goes to less than  $800^\circ \text{C}$ , the crystal transforms to a monoclinic structure ( $\beta''$ -phase) [3-9]. These alloys undergo transformations between the three different phases by changing the temperature, which is accompanied by changes in the electronic and elastic properties.

Few studies have been carried out on TaRu alloys [10].

However, to the best of our knowledge this is the first attempt to study the structural and electronic properties of TaRu alloys using ab-initio calculations.

In this work, we evaluate the angle of the monoclinic structure, which is not available experimentally, and calculate the elastic constants for the cubic structure.

This paper is prepared as follows: In section two, we present the method of calculation. In section three, we present the results and discussion and the conclusions are outlined in section four.

## 2. Computational Method

We performed self-consistent calculations using the full-potential linearized augmented plane wave (FP-LAPW) approach based on density functional theory (DFT) [11] as implemented in Wien2k [12]. In this method, the wave function, charge density and potential are expanded by spherical harmonic functions inside non overlapping spheres surrounding the atomic sites (muffin-tin spheres) and by a plane wave basis set in the remaining space of the unit cell (interstitial region). The calculated total energies are fitted to the Murnaghan equation of state [13] to obtain the energy-volume relation; and hence the lattice constants and bulk moduli are evaluated. The structures are fully relaxed using the damped Newton dynamics method to find the equilibrium atomic positions. The exchange correlation potential was treated using two methods: the generalized gradient approximation (GGA-PBE) [14] and local density approximation (LDA) [15].

The unit cells contain two atoms in the cubic CsCl structure ( $\beta$  phase), four atoms in the tetragonal  $L1_0$  ( $\beta'$  phase) and monoclinic structures  $B19'$  ( $\beta''$  phase). The calculations

Corresponding author:

amousa@meu.edu.jo (A. A. Mousa)

Published online at <http://journal.sapub.org/ajcmp>

Copyright © 2013 Scientific & Academic Publishing. All Rights Reserved

are performed with a  $(12 \times 12 \times 12)$  Monkhorst-Pack (MP)  $k$ -point mesh for the cubic structure (space group  $Pm\bar{3}m$ ), a  $(12 \times 12 \times 10)$  MP  $k$ -point mesh for tetragonal (space group  $P4/mmm$ ) and  $(8 \times 12 \times 8)$  MP  $k$ -point mesh for monoclinic structures (space group  $P2/m$ ), corresponding to 56  $k$  points in the  $\frac{1}{48}$ -irreducible BZ of the simple cubic cell, 105  $k$  points in the  $\frac{1}{16}$ -irreducible BZ of the tetragonal cell and 192  $k$  points in the  $\frac{1}{4}$ -irreducible BZ of the monoclinic cell. In each case, we performed geometrical optimization followed by self-consistent calculations to obtain the partial densities of states (DOS) for all structures using the tetrahedron method with Blöchl corrections[16].

The maximum quantum number  $\ell$  for the wave function expansion inside the atomic spheres is confined to  $\ell_{\max} = 10$ . The core cutoff energy is -81.66 eV and the plane wave cutoff,  $K_{\max} = 8/R_{\text{mt}}$  ( $R_{\text{mt}}$  is the smallest muffin-tin radius in the unit cell) is chosen for the expansion of wave functions in the interstitial region. The charge density is Fourier expanded up to  $G_{\max} = 12$ . The  $R_{\text{mt}}$  values for TaRu are chosen to be 2.2 a.u. for both Ta and Ru.

### 3. Results and Discussion

In this section we present the structural, electronic and elastic properties of TaRu binary alloys using GGA and LDA exchange-correlation potentials.

#### 3.1. Structural Properties and Phase Transformations

Tantalum-Ruthenium crystal has a CsCl-structure ( $\beta$ -phase) with a space group  $Pm\bar{3}m$  where Ta and Ru atoms are occupying the corners and the center of the cube. This material transforms martensitically from the parent phase ( $\beta$ ) to a monoclinic martensitic phase ( $\beta''$ ) with an intermediate tetragonal phase ( $\beta'$ ) at 1100° C[3-8]. From Table 1, one can see that the calculated lattice constants agree well with the experimental values[8].

In order to obtain the crystal structure of the  $\beta'$  phase, we deformed the CsCl-type structure of the  $\beta$  phase by continuously varying the  $c/a$  ratio, and keeping the volume

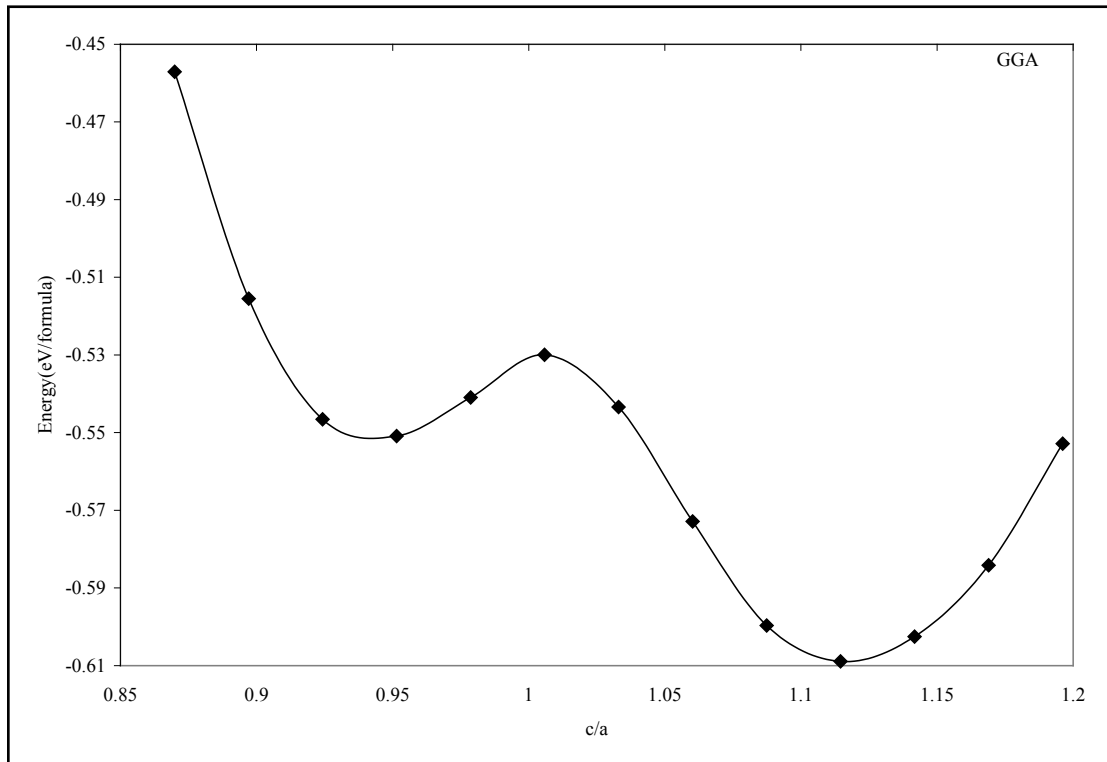
fixed at its optimal value. In Fig. 1 we present the relation of energy change versus the  $c/a$  ratio, where one can find two local minima at 0.94 (0.94) and 1.12 (1.13) using GGA (LDA) exchange-correlation potentials. The local minima at 1.12 (1.13) are lower in energy than the 0.94 minimum. This means that the cubic phase is unfavorable in energy as compared to the tetragonal phase, and undergoes two continuous tetragonal transformations. The  $\beta$  phase first undergoes cubic to tetragonal transformations with  $c/a = 0.94$ , and then with  $c/a = 1.12$  (1.13). Our results show that the optimal  $c/a$  for the  $\beta'$  phase is 1.12 (1.13), which is very close to the experimental value 1.09[5] and 1.12[10].

There is another transformation near 800° C that has been evidenced experimentally[7-9, 17], where the structure transforms to monoclinic ( $\beta''$  phase). The optimum volume of  $\beta''$  phase is found to be the same as the other two phases ( $\beta$ ,  $\beta'$ ). In addition to volume optimization, we optimized  $c/a$  and  $b/a$  ratios at constant volumes of 32 (30) Å<sup>3</sup> for GGA (LDA) exchange-correlation potentials, see Fig 2. Moreover, we optimized the  $\gamma$  angle for the  $\beta''$  phase, which is found to be 93° as can be seen in Fig.3. The final stage in building  $\beta''$  phase is by allowing the atoms to locate themselves in positions with minimum forces, i.e. finding the equilibrium positions of all individual atoms using a damped Newton dynamics method. In Table 2, we display the atomic positions for  $\beta''$  phase after relaxation.

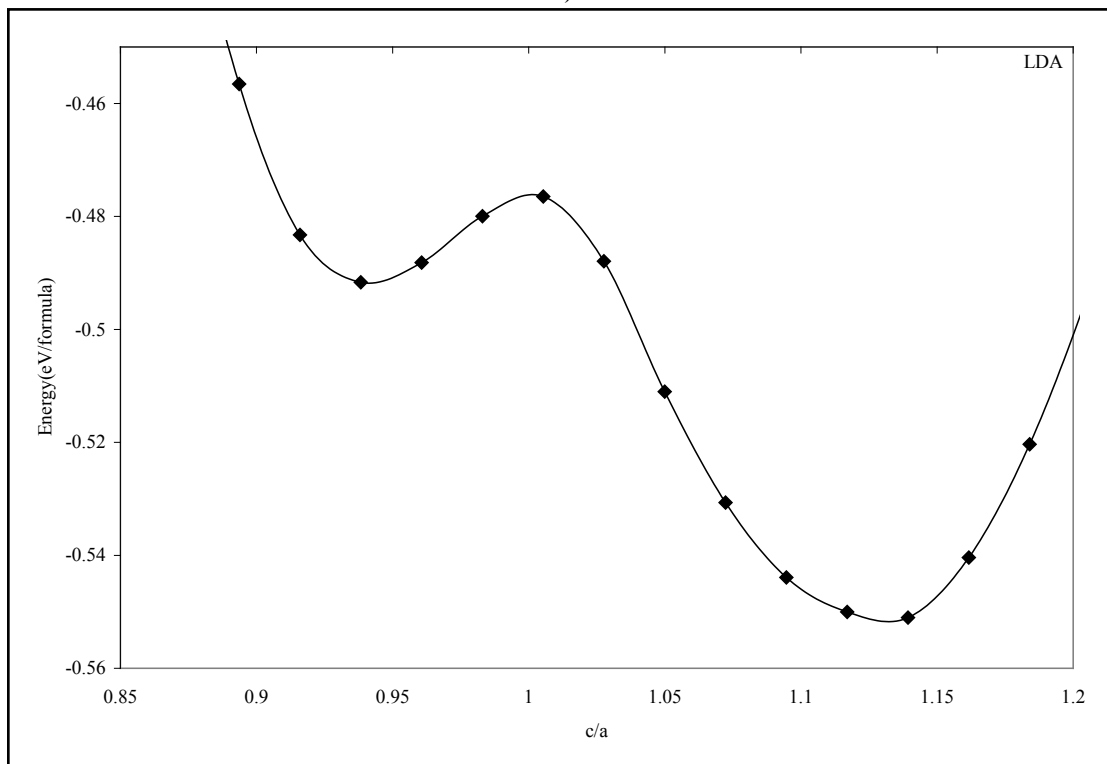
Furthermore, we performed geometrical optimization and a similar symmetry analysis to determine the crystal structure of the  $\beta'$  and  $\beta''$  phases. It is found that the  $\beta'$  phase has the  $P4/mmm$  space group with atomic positions: Ta (0, 0, 0), Ru (0.5, 0.5, 0.5) and  $\beta''$  has the  $P21/m$  space group with atomic position present in Table 2. The detailed lattice constants of the  $\beta'$  and  $\beta''$  phases are listed in Table 1, the calculated volume of three phases is about 32 Å<sup>3</sup>, and thus, the martensitic transformation involves almost no change in volume. This indicates that TaRu is a shape memory alloy, since volume conservation is a necessary and sufficient condition for the shape memory effect in transforming the system from a martensitic to cubic austenitic phase[18].

**Table 1.** Comparison between the calculated and experimental lattice parameters of TaRu  $\beta$ ,  $\beta'$  and  $\beta''$ - phases a) Ref (8) b) Ref (10)

		Present calculations		Experiment	Percentage Difference from experimental values (%)	
		LDA	GGA		LDA	GGA
$\beta$	a(Å)	3.11	3.17	3.19 <sup>a</sup>	-2.5	-0.6
$\beta'$	a(Å)	3.00	3.06	3.09 <sup>a</sup> , 3.05 <sup>b</sup>	-2.9	-1.0
	c(Å)	3.38	3.41	3.36 <sup>a</sup> , 3.39 <sup>b</sup>	0.6	1.5
$\beta''$	a(Å)	4.65	4.73			
	b(Å)	2.97	3.04			
	c(Å)	4.43	4.48			
	$\gamma^\circ$	93				



a)



b)

**Figure 1.** Total energy of  $\beta'$  phase as a function of  $c/a$  at optimal volume; GGA (a), LDA (b)

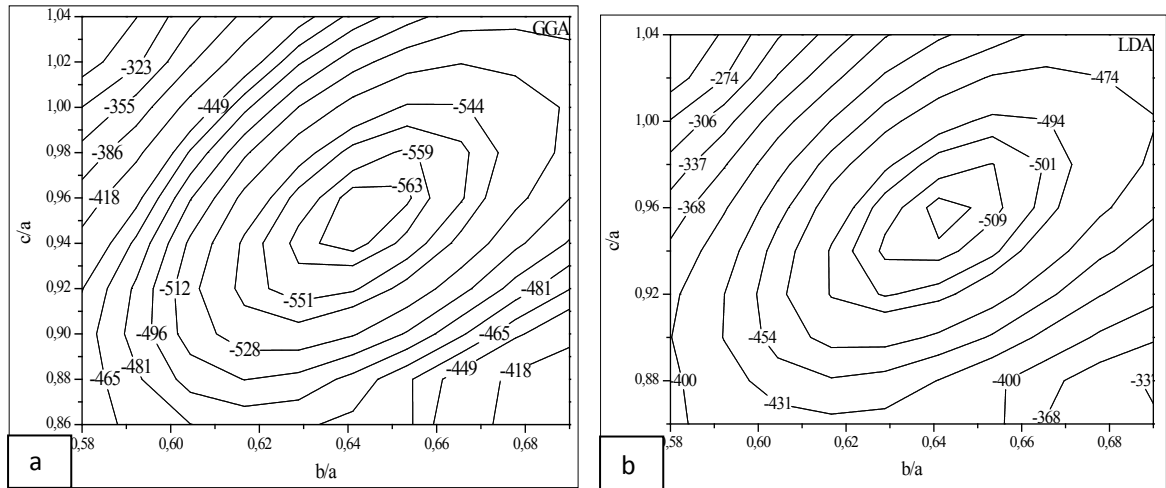


**Figure 2.** Total energy as a function of  $b/a$  and  $c/a$  for  $\beta$ "-phase; GGA (a), LDA (b)

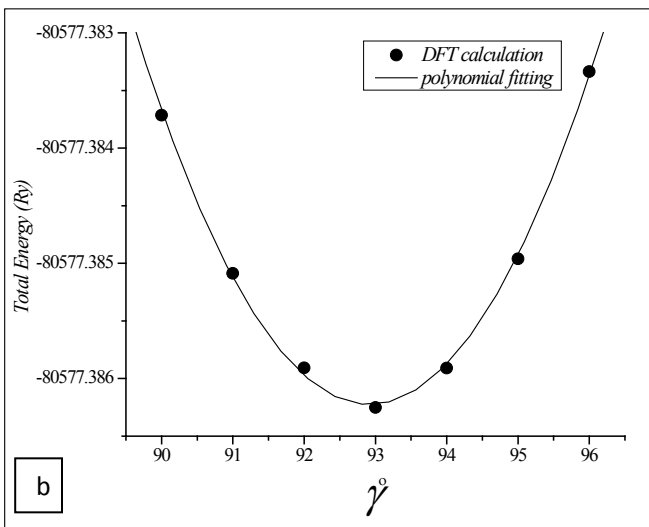
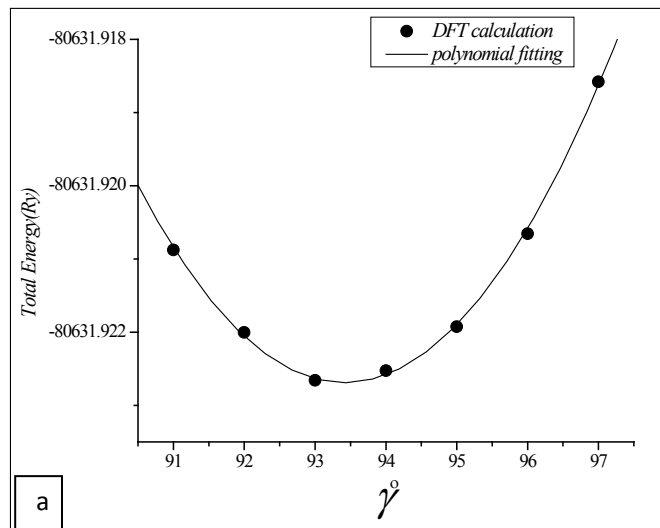


**Figure 3.** Total energy as a function of  $\gamma$ ; GGA (a), LDA (b)

**Table 2.** The atomic positions for monoclinic TaRu

Atom	x	y	z
Ta	0.269	0.476	0.250
	0.731	0.524	0.750
Ru	0.215	0.972	0.750
	0.785	0.028	0.250

### 3.2. Elastic Properties

The elastic properties play a key role in providing valuable information about structural stability and the binding characteristics between adjacent atomic planes. In general, there are only three independent elastic constants,  $C_{11}$ ,  $C_{12}$  and  $C_{44}$  for cubic crystals. To save the computation time, we have chosen three highly symmetrical types of deformation. The first type involves calculating the bulk modulus, which can be computed by the Birch-Murnaghan EOS[11]:

$$B(V_0) = V \left( \frac{\partial^2 E_{tot}}{\partial V^2} \right) \Big|_{V=V_0}, \quad (1)$$

which is related to the elastic constant as:

$$B = (1/3) (C_{11} + 2C_{12}) \quad (2)$$

The second deformation is a volume conservative tetragonal strain to calculate  $C_{11}$ - $C_{12}$ ; and the third deformation is a rhombohedral strain to deduce  $C_{11} + 2C_{12} + 2C_{44}$ . The associated strain tensors as well as the full set of equations, that relate the elastic constants to the strain-induced change in the total energy, can be found in Refs.[8,19].

The calculated elastic constants are listed in Table 3 for  $\beta$ -phase. The bulk modulus is calculated from the theoretical values of the elastic constants using equation (2). This value is nearly the same as the one obtained from the structure optimization using Murnaghan fit equation of state[9] with 249 (283) GP for GGA (LDA). The bulk modulus ( $B(V_0)$ ) in GGA is less than that using LDA. This is related to the fact that the volume of the unit cell ( $V_0$ ), using GGA, is found to be larger than that of LDA.

These elastic constants can be used as an indicator of the stability of the cubic phase using Born's mechanical stability conditions[20, 21] as follows:

$$C_{11} + 2C_{12} > 0 \text{ or } B > 0 \quad (3-a)$$

$$C_{11} > 0 \quad (3-b)$$

$$C_{44} > 0 \quad (3-c)$$

$$C_{11} - C_{12} > 0 \quad (3-d)$$

In Table 3 one can see that the first three conditions are satisfied, but the fourth mechanical stability condition is violated, this means that the  $\beta$  phase is mechanically unstable.

**Table 3.** The calculated values of the elastic constants (GPa) and bulk modulus (GPa) of the TaRu  $\beta$ -phase

	$C_{11}$ (GPa)	$C_{12}$ (GPa)	$C_{44}$ (GPa)	B (GPa)
GGA	191	265	44	240
LDA	230	299	39	276

Our results here for TaRu alloy are consistent with our previous work of NbRu alloy as they both have structural transformation from  $\beta$  to  $\beta'$  and from  $\beta'$  to  $\beta''$  at 1100°C and 800°C for the former and 900°C and 750°C for the latter[22].

### 3.3. Energetic Properties

We also calculated the formation energies for different structures by subtracting the weighted sum of the total energies of the constituent elements (Ta in fcc structure and Ru in hcp structure) from the total energy of the compound as[23]:

$$\Delta E = E_{Ta_aRu_b} - (aE_{Ta}^{fcc} + bE_{Ru}^{hcp}), \quad (4)$$

where  $E_{Ta}$  and  $E_{Ru}$  are the total energies per atom for Ta and Ru elements, respectively;  $a$  and  $b$  correspond to the number of atoms for each constituent in the compound, and

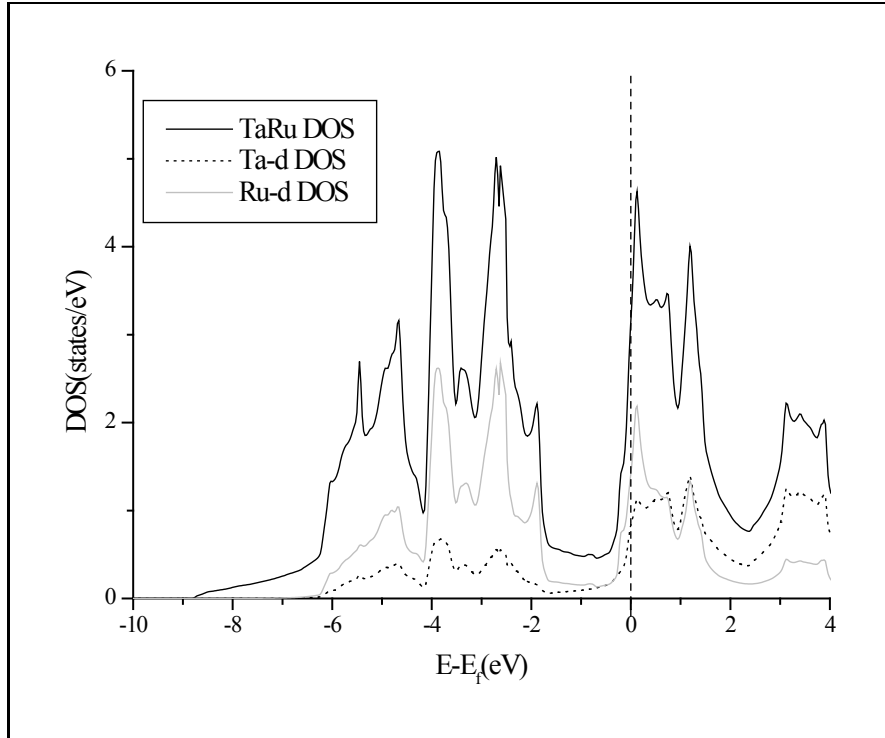
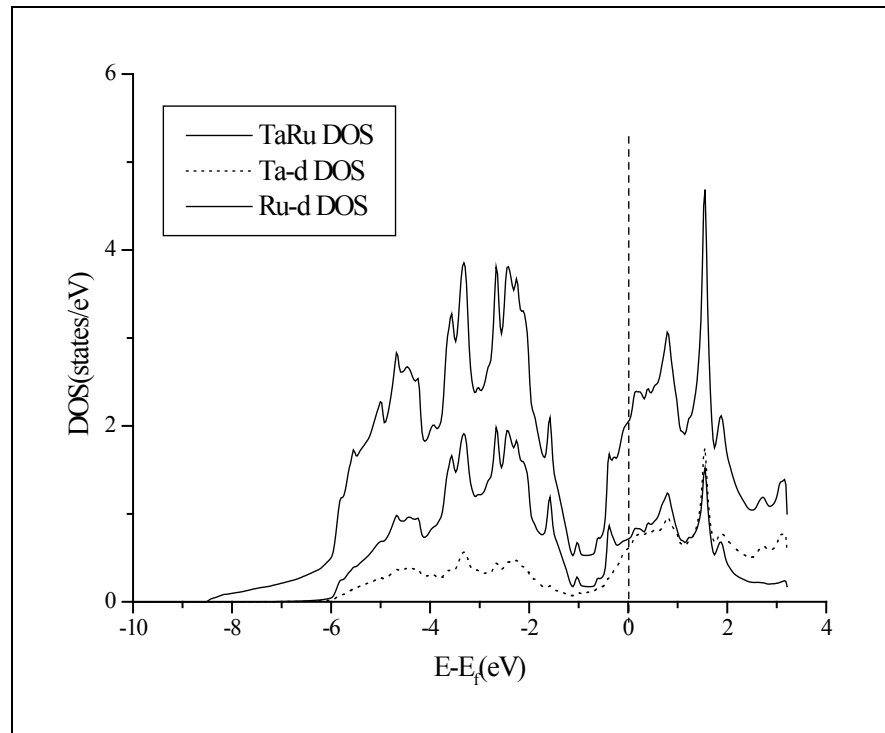
$E_{Ta_aRu_b}$  is the total energy of the compound per formula unit. The ground state is calculated relative to the  $\beta$ -phase, see Table 4. By comparing the formation energies of the three phases, we find that the  $\beta''$ -phase is the ground state with the lowest formation energy.

**Table 4.** The ground-state and formation energies for the three phases of TaRu. The ground-state energy is relative to  $\beta$  phase

	Ground state energy (meV/formula)		Formation energy (meV/formula)	
	GGA	LDA	GGA	LDA
$\beta$ -phase	0	0	-529.8	-475.4
$\beta'$ -phase	-75.0	-77.0	-604.8	-552.4
$\beta''$ -phase	-84.3	-85.9	-614.1	-561.3

### 3.4. Electronic Properties

To better examine the differences in the studied crystal structures, we plot the density of states (DOS) for  $\beta$ -phase,  $\beta'$ -phase and  $\beta''$ -phase in Fig.4. From this figure we note that the peaks of the  $\beta''$ -phase are the broadest among the three phases followed by the peaks of the  $\beta'$ -phase and then the  $\beta$ -phase. This can be ascribed to the fact that the  $\beta''$ -phase has a lowest symmetry as compared to  $\beta'$ -phase and finally  $\beta$ -phase. One can notice as well that total  $\beta''$ -phase has the lowest DOS at the Fermi level  $E_F$  followed by that of  $\beta'$ -phase and finally that of  $\beta$ -phase. This could be used as an indication that the  $\beta''$ -phase is the most stable one[21]. Our calculations agree well with previous experimental results[3-6]. From this figure one can also notice that the total DOS below  $E_F$  are mainly dominated by the Ru-d state, while the DOS above  $E_F$  are mainly the Ta-d state. We find that the difference between Ru-d DOS and Ta-d DOS in  $\beta''$ -phase is very small as compared to the other two phases, so that the hybridization between Ta-d state and Ru-d state in  $\beta''$ -phase is the strongest among the three phases. In contrast,  $\beta$ -phase has the weakest hybridization.

a)  $\beta$ -phasesb)  $\beta'$ -phases

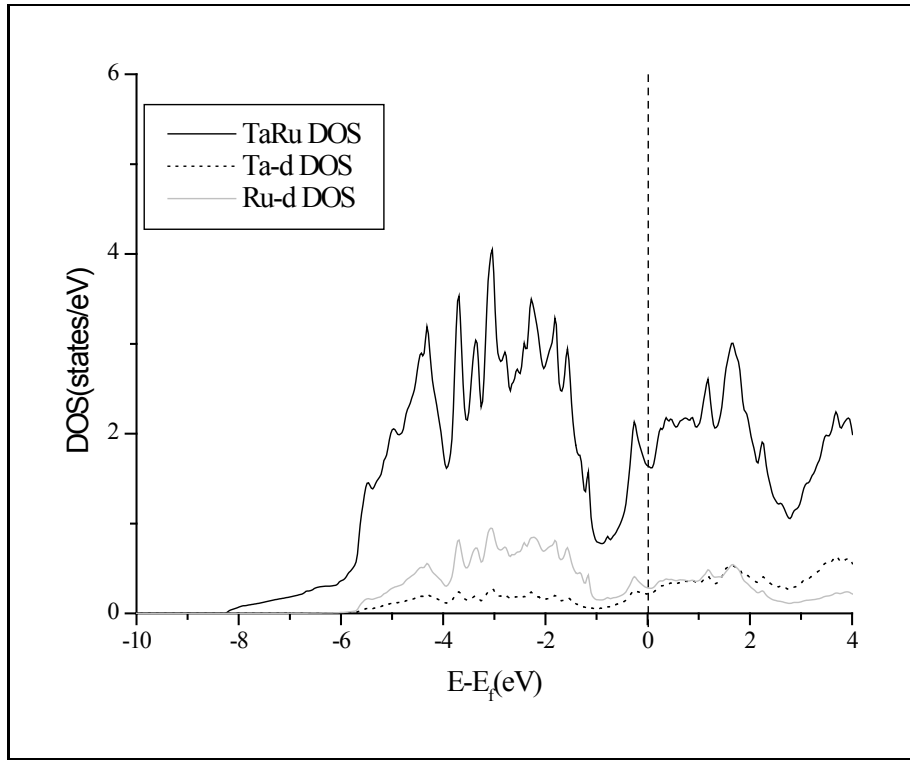


**Figure 4.** Total and partial DOS for  $\beta$  (a),  $\beta'$  (b) and  $\beta''$ -phases(c)

In Fig 5 we plot DOS at  $E_F$  [ $N(E_F)$ ] versus formation energy for the three phases. One can see that the level of  $N(E_F)$  gives an indication to the stability of the structures. So the lower is its level at  $E_F$  the lower is the formation energy, which means a more stable structure.

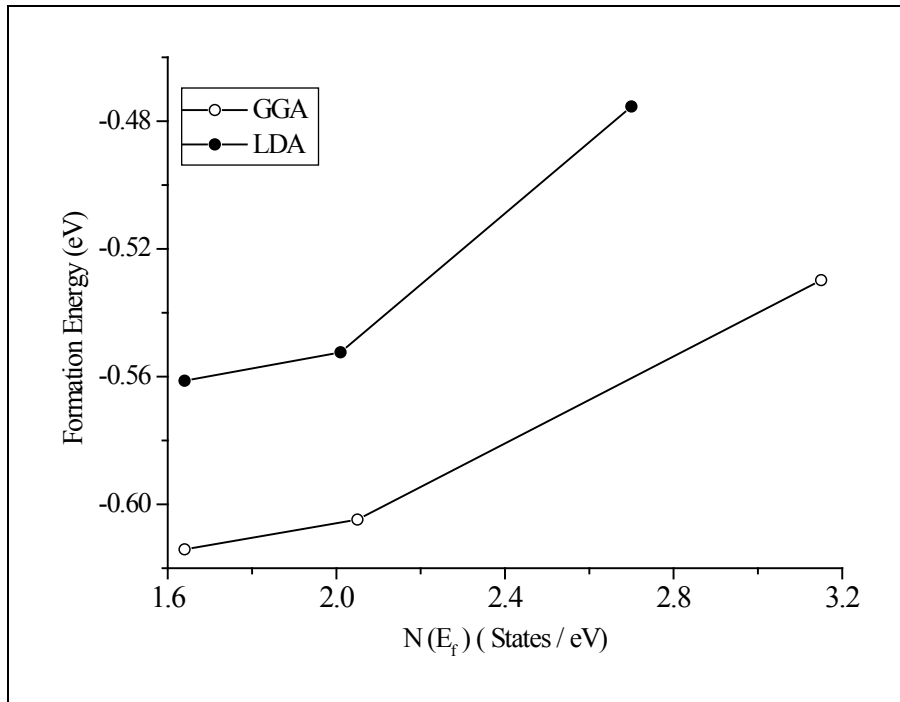


**Figure 5.** Total DOS at  $E_f$  versus the formation energy for  $\beta$ ,  $\beta'$  and  $\beta''$ -phases

## 4. Conclusions

The main conclusions of this work can be summarized as follows:

1. we put in evidence that the low-temperature ground-state structure is the  $\beta''$ -phase, which is found to be more stable than the tetragonal  $\beta'$ -phase and the cubic  $\beta$ -phase.
2. Our calculations show that the  $\beta''$ -phase has a monoclinic structure of (P21/m) symmetry.
3. The calculated DOS shows that the hybridization between Ta “d” and Ru “d” states is responsible for the phase stability of TaRu.
4. Our GGA calculations are found to be in a better agreement with the available experimental values [8, 10] than LDA.
5. The Born’s mechanical stability condition,  $C_{11}-C_{12} > 0$ , is not satisfied for  $\beta$ -phase due to the instability of this phase at low temperatures.

## ACKNOWLEDGEMENTS

The author thanks the staff at the theoretical physics laboratory of the University of Jordan.

## REFERENCES

- 
- [1] S. M. Shapiro, G. Xu, G. Gu, J. Gardner, R. W. Fonda, *Phys. Rev. B* 73, 214114 (2006).
  - [2] J. Beyer and J. H. Mulder, *Mater. Res. Soc. Symp. Proc.* 360, 443 (1995).
  - [3] G. S. Firstov, J. V. Humbeeck and Y. N. Koval, *Journal of Intelligent System and structures* 17, 1041 (2006).
  - [4] J. Ma, I. Karaman and R. D. Noebe *International, Materials Reviews* (2010), 55, 5
  - [5] M. Imran Khan, Hee Young Kim, Tae-hyun Nam, Shuichi Miyazaki, *Acta Materialia*, **60** 16, (2012), 5900–5913
  - [6] K. Chastaing, A. Denquin, R. Portier, P. Vermaut, *Materials Science and Engineering: A*, 481–482, 2008, 702–706
  - [7] R.W. Fonda, H.N. Jones, and R.A. Vandermeer, *Scripta Materialia* 3, 1031 (1998).
  - [8] R. W. Fonda and R. A. Vandermeer, *Philosophical Magazine A* 76, 119 (1997).
  - [9] X. GAO, Y. ZHENG, W. CAI, S. ZHANG and L. ZHAO, *J. Mater. Sci. Technol.*, 2004, 20(1).
  - [10] T. Tsukamoto, K. Koyama, A. Oota, S. Noguchi, *Cryogenics* 28 (1988) 580–584.
  - [11] P. Hohenberg and W. Kohn, *Phys. Rev. B*, 1964, 136, 864.
  - [12] P. Blaha, K. Schwarz, and J. Luitz, *Wien2k, A Full Potential Lineared Augmented Plane Wave Package for Calculating Crystal Properties* (Kalheinz Schwarz, Techn. Universitat Wien, Austria).
  - [13] F. D. Murnaghan, *Proc. Natl. Acad. Sci. (U.S.A.)*, 1994, 30, 244.
  - [14] J. P. Perdew, S. Burke, M. Ernzerhof, *Phys. Rev. Lett.*, 1996, 77, 3865.
  - [15] J. P. Perdew and A. Zunger, *Phys. Rev. B.*, 1981, 23, 5048.
  - [16] P. E. Blöchl, O. Jepsen, and O. K. Andersen, *phys. Rev. B.*, 1994, 49, 16223.
  - [17] H. Okamoto, *J. Phase Equilib.*, 1991, 12, 395.
  - [18] K. Bhattacharya, *Microstructure of Martensite*, Oxford University Press, Oxford, 2003.
  - [19] T. Charpin, A package for calculating elastic tensor of a cubic phases using WIEN, *Laboratoire Des Géomatériaux de l’IPGP*, 4, p1 Jussieu, F-75252 Paris, 2001.
  - [20] J. Wang, S. Yip, S. R. Phillpot and D. Wolf, *Phys. Rev. Lett.*, 1993, 71, 4182.
  - [21] V. Shpakov, J. S. Tse, V. R. Belosludov, and R. V. Belosludov, *J. Pys: Condens. Matter*, 1997, 9, 5853.
  - [22] A. A. Mousa, B. A. Hamad, and J. M. Khalifeh, *Eur. Phys. J. B* 72, 575 (2009).
  - [23] M. Sanati, R. C. Albers, F. J. Pinski, *Phys. Rev. B*, 1998, 58, 13 590.
  - [24] Y. Y. Ye, C. T. Chan, K. M. Ho, *Phys. Rev. B*, 1997, 56, 3678.